Electronic Supplementary Information for

A unique strategy for preparing single-phase unitary/binary oxides-graphene composites

Kuo-Hsin Chang,[a,b] *Ying-Feng Lee,*[a] *Chi-Chang Hu,*[a,]* *Chih-I Chang,*[a] *Chien-Liang Liu*[a] *and Yi-Lin Yang*[b]

a. Department of Chemical Engineering, National Tsing Hua University, Hsin-Chu 30013, TAIWAN
b. Department of Chemical Engineering, National Chung Cheng University, Chia-Yi 62102, TAIWAN
* To whom correspondence should be addressed. E-mail: cchu@che.nthu.edu.tw

This supporting information includes Figures S1 – S11 and experimental method.

(1) TiO_2/GS and SnO_2/GS prepared by MAH (Route 1):

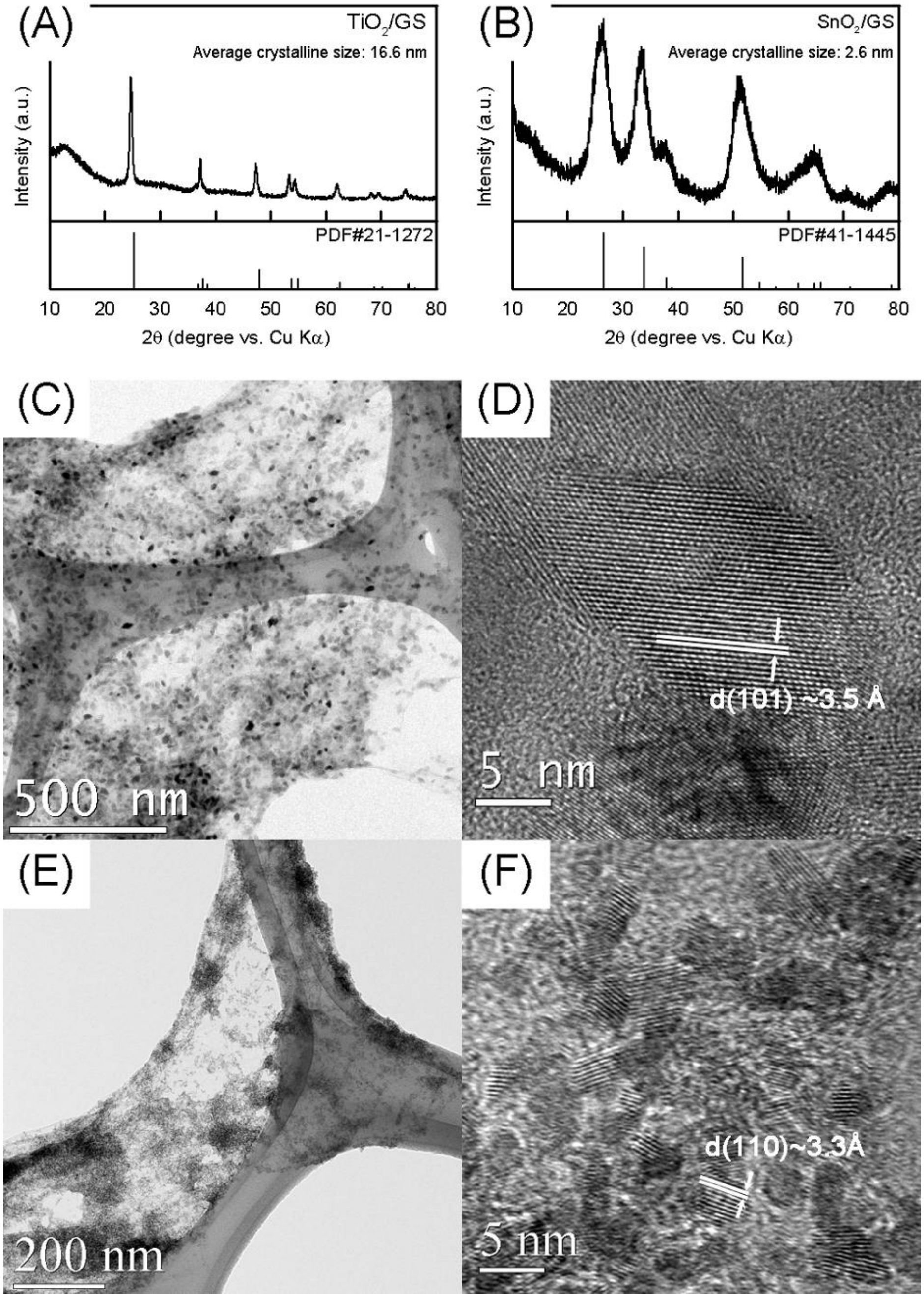

Fig. S1 (A,B) XRD patterns, (C,E) bright-field and (D,F) HR-lattice TEM images of (A,C,D) anatase TiO_2/GS and (B,E,F) SnO_2/GS nanocomposites prepared by means of a microwave-assisted hydrothermal synthesis at 200°C for 5 min (route 1 in **Scheme 1**). The XRD peaks well match with their standard patterns and the clear d-spaces equal to 0.35 and 0.33 nm in HR-lattice images are respectively indexed as the (101) face of anatase TiO_2 and (110) face of SnO_2. This figure clearly shows that TiO_2/GS and SnO_2/GS composites are easily obtained by normal one-step microwave-assisted hydrothermal synthesis from the precursor solution containing GO and metallic ions.

(2) The mechanism of hydrothermal synthesis:

The reasons why the same hydrothermal synthesis does not work with certain inorganic salt precursors are briefly discussed here from the mechanism viewpoint of hydrothermal synthesis.

Note that the potential-pH diagram of elements can be employed as a reference for the formation and crystallization of transition metal oxides although the potential-pH diagrams of elements under the hydrothermal environment are different from those observed at 25^{o}C. In our opinion, crystallization of metal oxides through hydrothermal synthesis can be simply classified into two types on the basis of their potential-pH diagrams [2], such as Fig. S2. In Fig. S2(A), some oxides, such as Ti oxide, Sn oxide, Ru oxide, and so on, dominate over other species in their potential-pH diagrams. These oxides can be easily prepared by hydrothermal synthesis with their inorganic salt precursors from the thermodynamic viewpoint. In Fig. S2(B), however, certain oxides, such as Mn oxide, Ni oxide, Co oxide, and so on, are only thermodynamically stable in the high-pH region or the highly positive potential region. Therefore, to promote the formation and crystallization of this kind of oxides, adding urea to increase the pH of precursor solution or adding the oxidizer to increase the oxidation state of metallic ions during the hydrothermal reaction are necessary. On the other hand, in our previous study, Mn oxides can be directly prepared by using its acetate salt precursor [3]. This phenomenon is attributable to the relatively low oxidation potential of acetate salt precursor, resulting from the formation of Mn–AcO complexes [4]. The relatively low oxidation potential means that metallic ions of the acetate salt precursors are more easily oxidized to those under higher oxidation states, favorably forming oxides in comparison with the other inorganic salt precursors. This idea is under investigation in this lab. Unfortunately, much larger crystals were obtained by using the acetate salt precursor through the hydrothermal method [3], which are undesirable in energy storage/conversion systems.

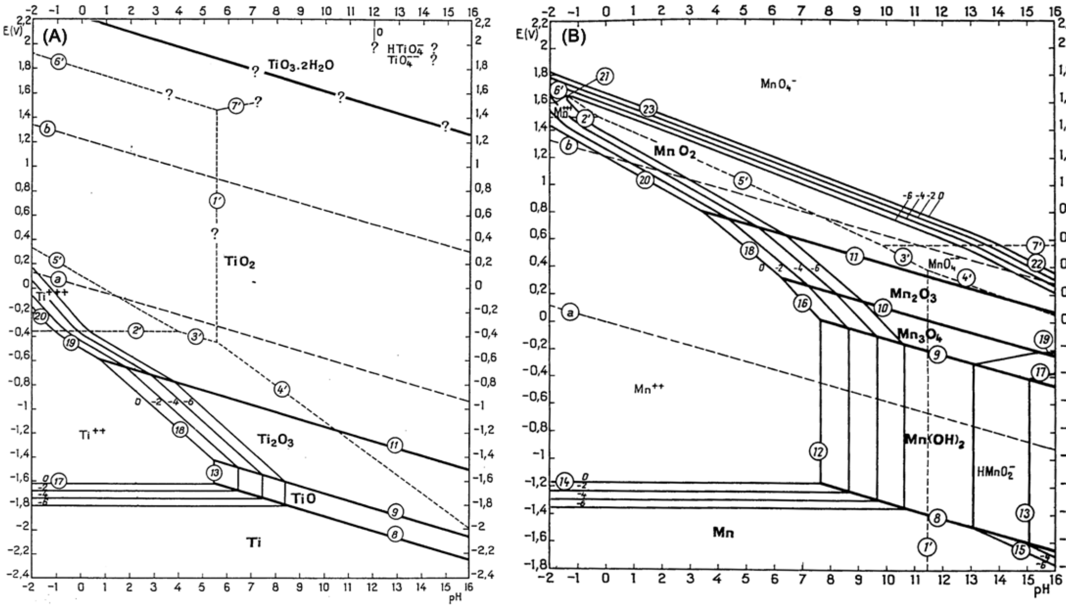

Fig. S2 Potential-pH equilibrium diagram for the aqueous system of (A) Ti and (B) Mn elements [2].

[1] A. Rabenau, *Angew. Chem. Int. Ed.*, 1985, **24**, 1026.

[2] M. Pourbaix, *Atlas of Electrochemical Equilibria in Aqueous Solutions*, NACE, Houston, Texas (1974).

[3] C.C. Hu, Y.T. Wu, K.H. Chang, *Chem. Mater*, 2008, **20**, 2890.

[4] C.C. Hu, P.Y. Chuang, Y.T. Wu, *J. Electrochem. Soc.*, 2005, **152**, C723.

(3) Mn oxide prepared by MAH (Route 1) from the acetate precursors or via the urea hydrolysis method:

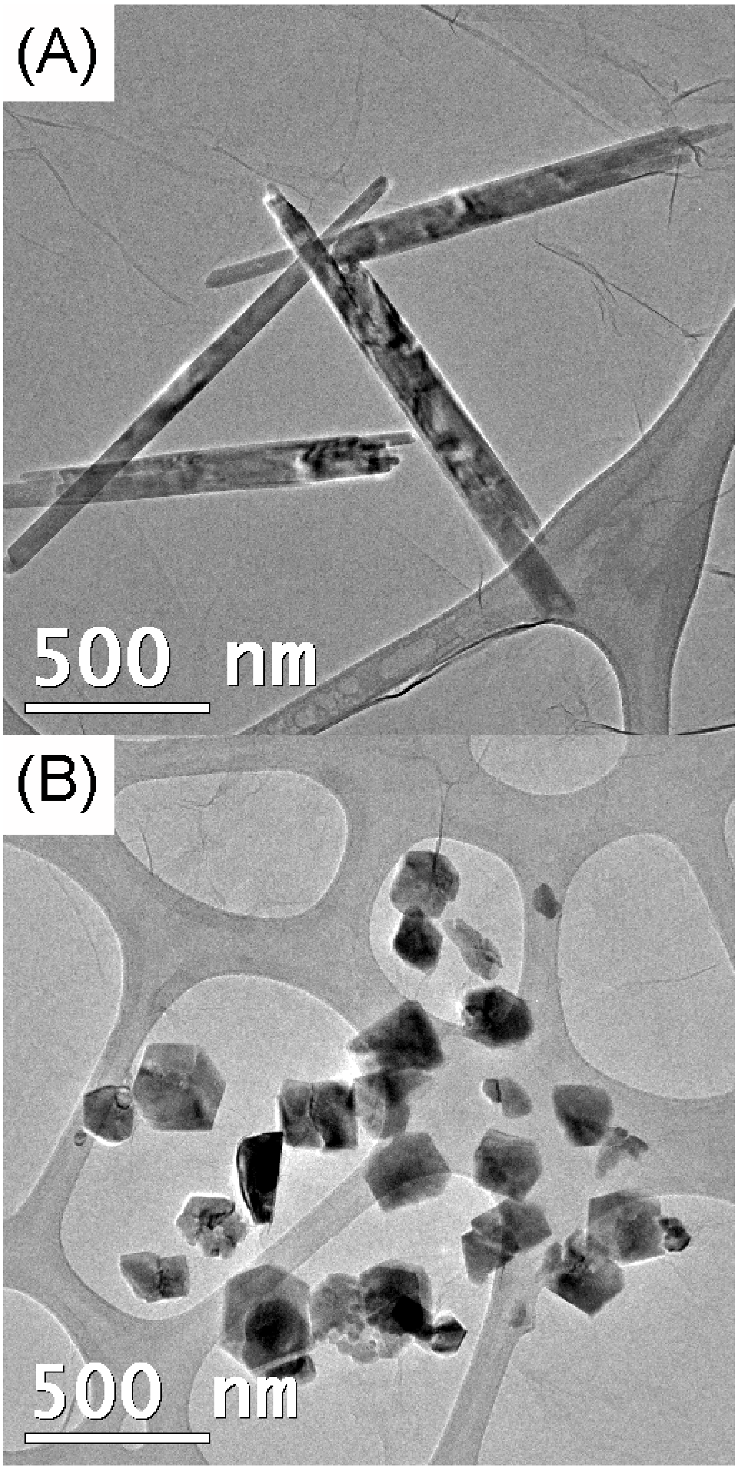

Fig. S3 Bright-field TEM images of (A) MnOOH/GS and (B) Mn_3O_4/GS prepared by the normal one-step microwave-assisted hydrothermal synthesis at 200^oC for 5 min through using (A) the acetate precursors and (B) the urea hydrolysis methods. Clearly, the crystalline size of manganese oxides prepared by the above methods is too large to uniformly disperse the oxides on the GS surface.

(4) TiO_2/GS and SnO_2/GS prepared by microwave-assisted hydrothermal annealing (Route 2):

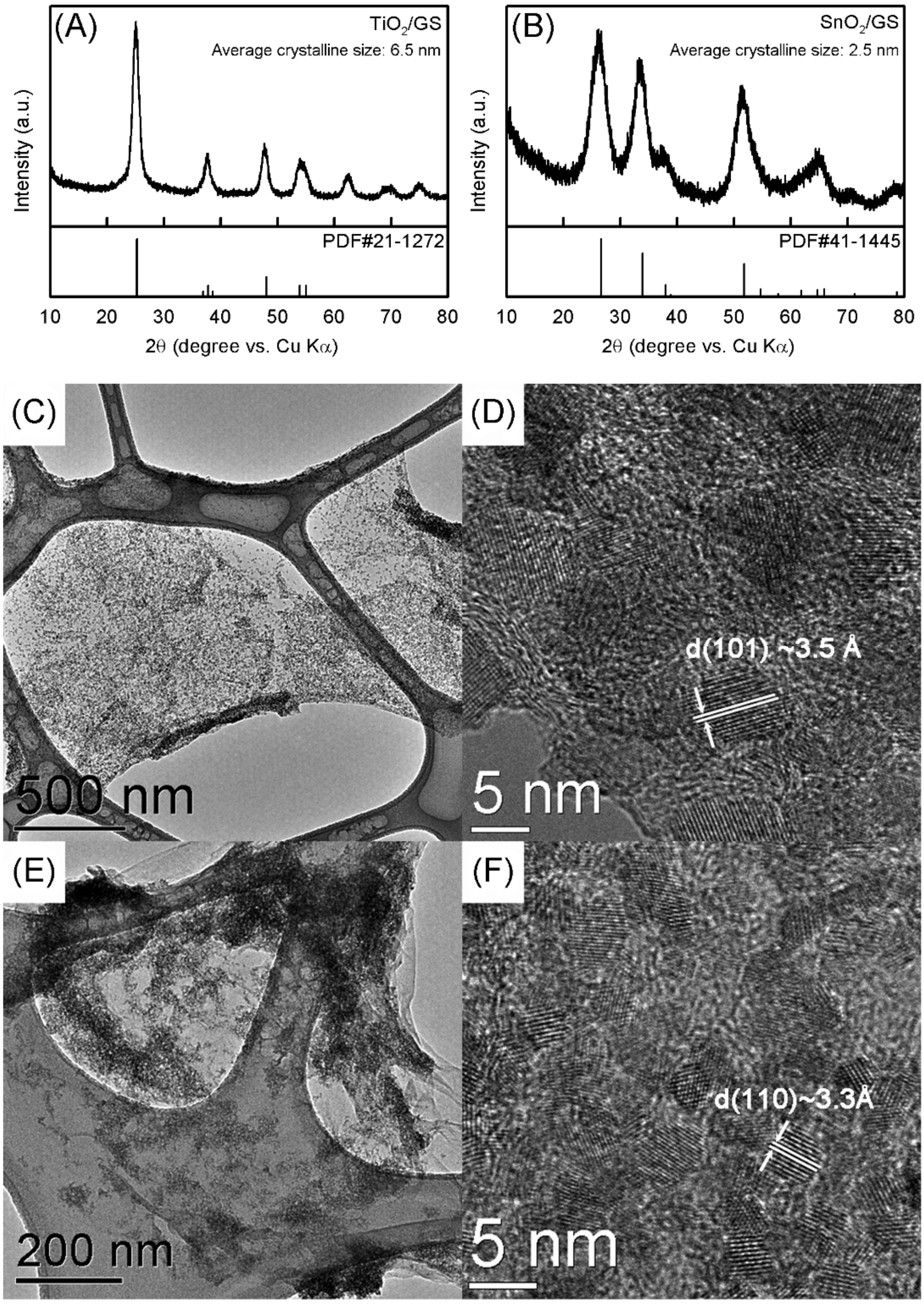

Fig. S4 (A,B) XRD patterns, (C,E) bright-field and (D,F) HR-lattice TEM images of (A,C,D) anatase TiO_2/GS and (B,E,F) SnO_2/GS composites prepared by means of the two-step strategy with microwave-assisted hydrothermal annealing at 200°C for 5 min (route 2 in **Scheme 1**). This figure clearly shows that TiO_2/GS and SnO_2/GS nanocomposites can be prepared by the two-step process: (1) forming the hydroxide/GO mixtures and (2) applying the microwave-assisted hydrothermal annealing.

(5) TiO_2/GS and SnO_2/GS prepared by microwave-assisted solvothermal annealing (Route 2):

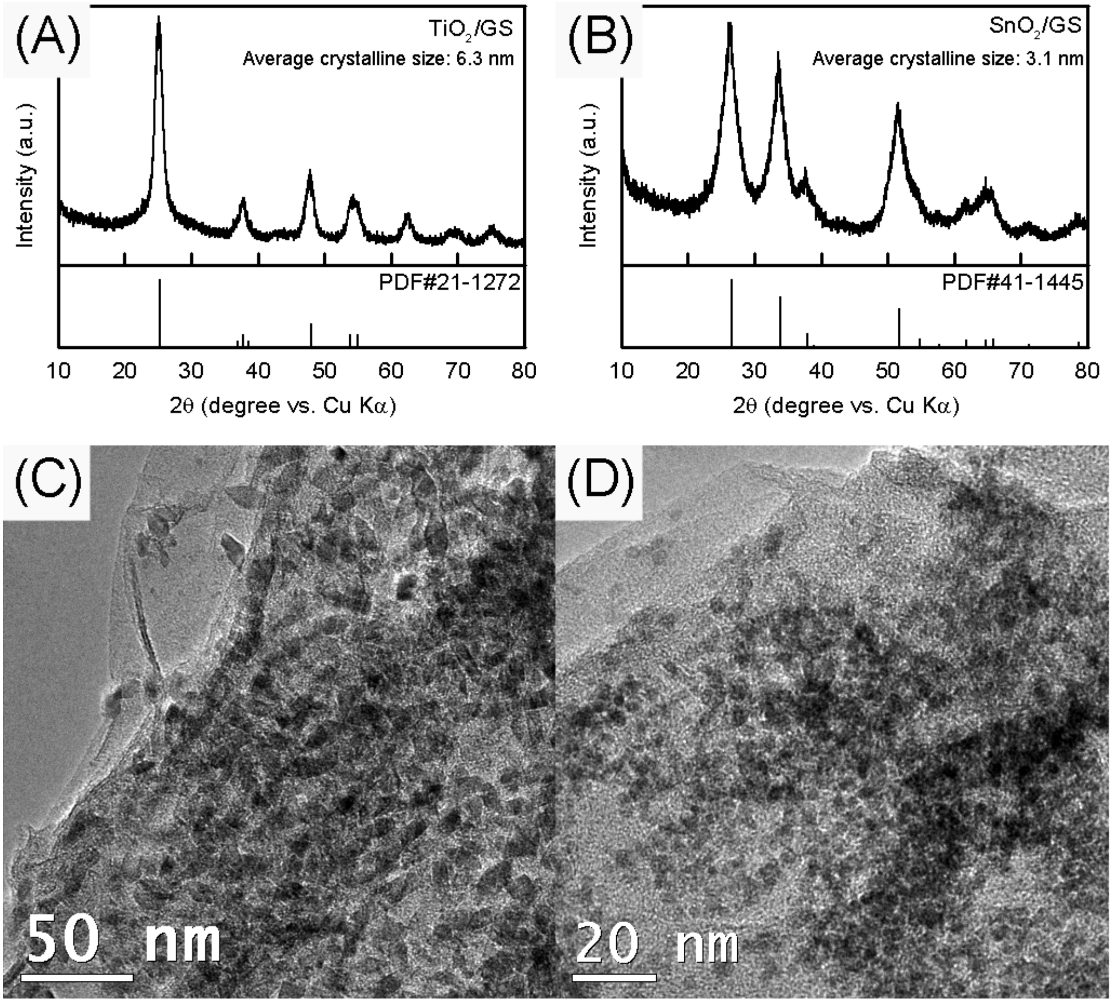

Fig. S5 (A,B) XRD patterns and (C,D) bright-field TEM images of (A,C) anatase TiO_2/GS and (B,D) SnO_2/GS composites prepared by means of the two-step strategy with microwave-assisted solvothermal annealing at 200°C for 5 min (route 2 in **Scheme 1**). This figure clearly shows that TiO_2/GS and SnO_2/GS nanocomposites can be prepared by the two-step process: (1) forming the hydroxide/GO mixtures and (2) applying the microwave-assisted solvothermal annealing.

(6) Zn_2SnO_4/GS prepared by microwave-assisted hydrothermal annealing (Route 2):

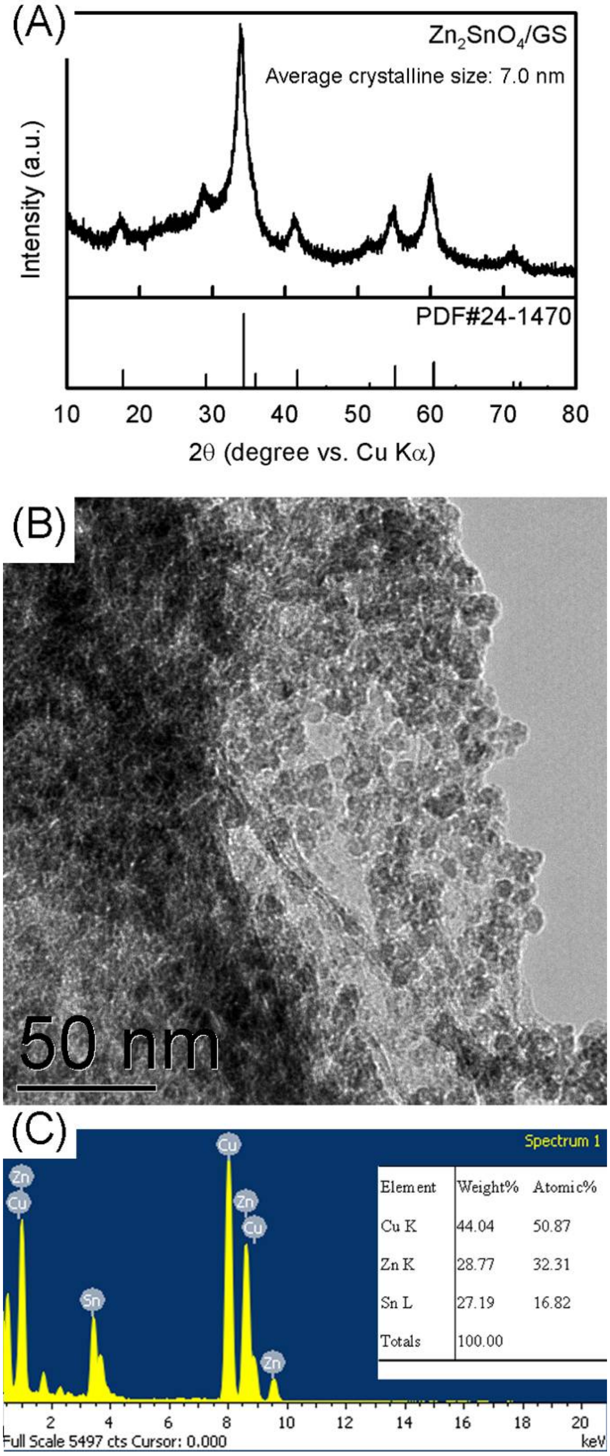

Element	Weight%	Atomic%
Cu K	44.04	50.87
Zn K	28.77	32.31
Sn L	27.19	16.82
Totals	100.00	

Fig. S6 (A) An XRD pattern, (B) a bright-field TEM image, and (C) an EDX spectrum of Zn_2SnO_4/GS nanocomposites prepared by means of the two-step process with the microwave-assisted hydrothermal annealing at 200°C for 5 min. From the successful preparation of single-phase binary oxides, the additional novelty of the two-step strategy proposed in this work has been clearly exhibited.

(7) (Ru-Sn)O_2/GS prepared by microwave-assisted hydrothermal annealing (Route 2):

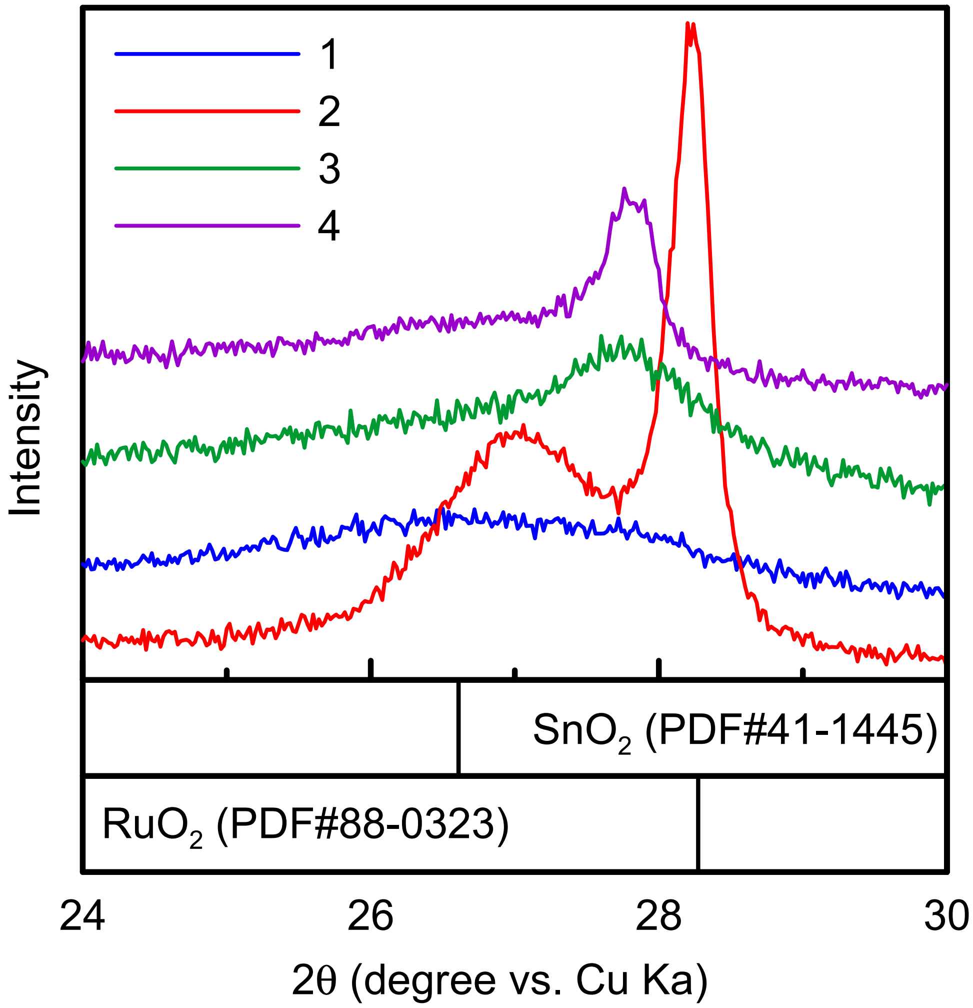

Fig. S7 XRD patterns of annealed samples for (1,2) RuO_2-SnO_2 mixtures and (3,4) solid-solution (Ru-Sn)O_2/GS nanocomposites prepared by means of the two-step process with the microwave-assisted hydrothermal annealing at 150°C for 5 min and with post-annealing treatment at (1,3) 250°C and (2,4) 800°C in air. Note the molar ratio of Ru/Sn is equal to 1, and the post-annealing treatment of all samples in air was carried out because the crystalline size of as-prepared samples is too small to be identified by XRD analyses. From comparison all XRD patterns, two-phase RuO_2/(Ru-Sn)O_2 solid-solution mixtures were clearly found from the hydroxides without GO. However, (Ru-Sn)O_2 solid-solution is easily obtained by heating the mixture of GO-fixed hydroxides via microwave-assisted hydrothermal annealing. The above results clearly prove the unprecedented approach for rapidly preparing the single-phase unitary/binary/solid-solution oxides-graphene composites at low temperatures by our proposed method.

(8) Capacitive performances of Mn_3O_4 and Mn_3O_4/GS:

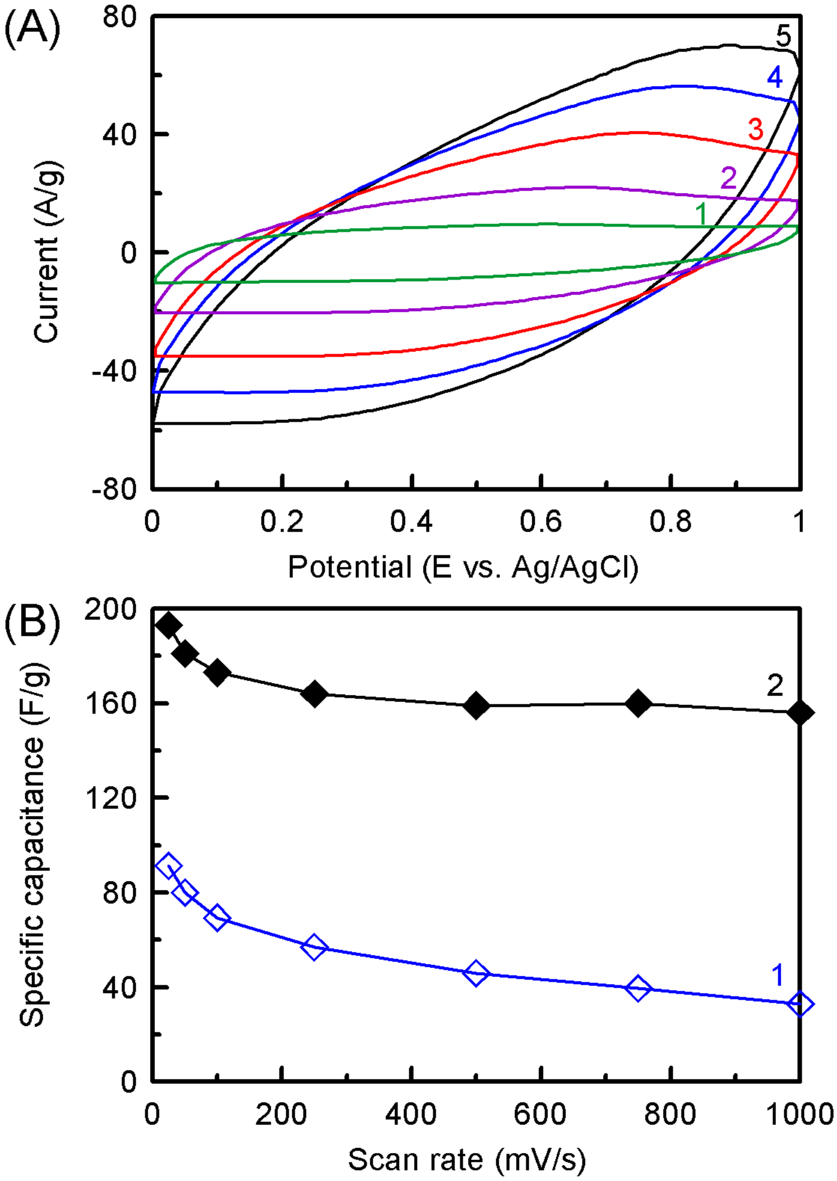

Fig. S8 (A) CVs of a Mn_3O_4-coated electrode measured at (1) 100, (2) 250, (3) 500, (4) 750, and (5) 1000 mV/s in 1 M Na_2SO_4. The CV responses clearly show the poor capacitive performances of a Mn_3O_4-coated electrode under high scan rates of CV. (B) Dependence of specific capacitance on scan rate for (1) Mn_3O_4 electrode and (2) Mn_3O_4/GS electrode. The capacitive performances of Mn_3O_4 are significantly enhanced by adding GS into Mn_3O_4.

(9) Sensing ability of $NiCo_2O_4$/GS:

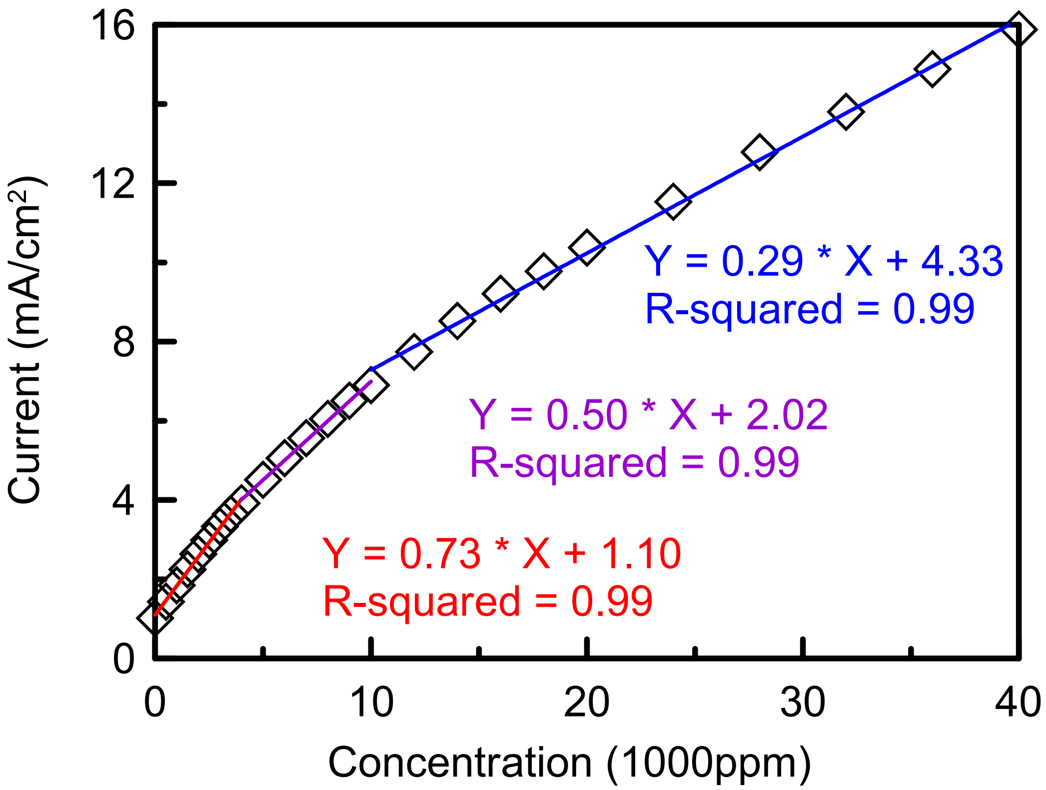

Fig. S9 Dependence of the oxidation current density at 0.5 V on the concentration of methanol. Note that this plot was obtained from the LSV responses in Figure 3D. This plot reveals that $NiCo_2O_4$/GS is a promising next-generation electrode material for an alcohol sensor with high activity and a wide-concentration sensing range.

(10) Experimental method

Nano graphite platelets (N008-100-N) with ca. 100 nm in thickness, purchased from Angstron Materials Co. (USA), were used as the raw materials to prepare GO. The preparation of GO nanosheets generally follows the modified Hummers' method with the supersonic exfoliation. Note the average thickness of GO sheet equal to ca. 0.74 nm (see Fig. S10), reveals that isolated single-layer GO was successfully prepared in this work. The XPS analyses of GO and reduced GO (see Fig. S11) were carried out to confirm the rapidly reduction of GO by microwave-assisted hydrothermal treatment at 200^{o}C for 5 min. For preparation of oxide crystallites/GS nanocomposites, the precursor solution of metal chloride was well mixed with GO solution for 10 min before the microwave-assisted treatment. For route 1, the mixture was directly heated from room temperature to 200^{o}C and kept at the specified temperature with an air-flow cooling for 5 min at a constant power (i.e., under the PowerMax mode) of 100 W in a microwave reactor (Discover, CEM). For route 2, the hydroxide/GO mixture was obtained after adding 1M NaOH solution into the solution consisting of metal ions and GO. The hydroxide/GO mixture was exposed by the same microwave-assisted procedure. For microwave-assisted solvothermal annealing, hydroxide/GO mixture was ultrasonically dispersed into DMF solvent after collecting by a centrifuge. After the microwave-assisted solvothermal annealing step, the resultant oxide/graphene nanocomposites were obtained by filtration through a PTFE membrane with the pore size of 0.4 μm. The filtered powders were washed several times by deionized water, and dried in a vacuum oven at 85°C overnight.

For preparing oxide/graphene-coated electrodes, the electrode materials with 10 % binder of PVDF were dispersed in MNP solvent for 10 min to form the coating ink. The ink was dropped onto the surface of pre-polished graphite substrates (1 cm^2) to form the working electrodes. Finally, these electrodes were dried in a vacuum oven at 85°C overnight. The thickness of GO was identified by an atomic force microscope (AFM, Digital Instrument D3100). The crystalline structure of oxides was identified by means of an X-ray diffractometer (Ultima IV, Rigaku) using a Cu target (CuKa = 1.5418 Å) at an angle speed of 1^{o} (2θ) min^{-1}. The microstructure of oxides and GS were examined by means of a field-emission transmission electron microscope (FE-TEM, Philips Tecnai). Electrochemical characteristics were obtained by an electrochemical analyzer system, CHI 633A (CH instruments, USA) in a three-compartment cell. An Ag/AgCl electrode was used as the reference and a piece of platinum gauze was employed as the counter electrode. All solutions used in this work were prepared with 18MΩ-cm de-ionized water produced by a reagent water system (Milli-Q SP, Japan).

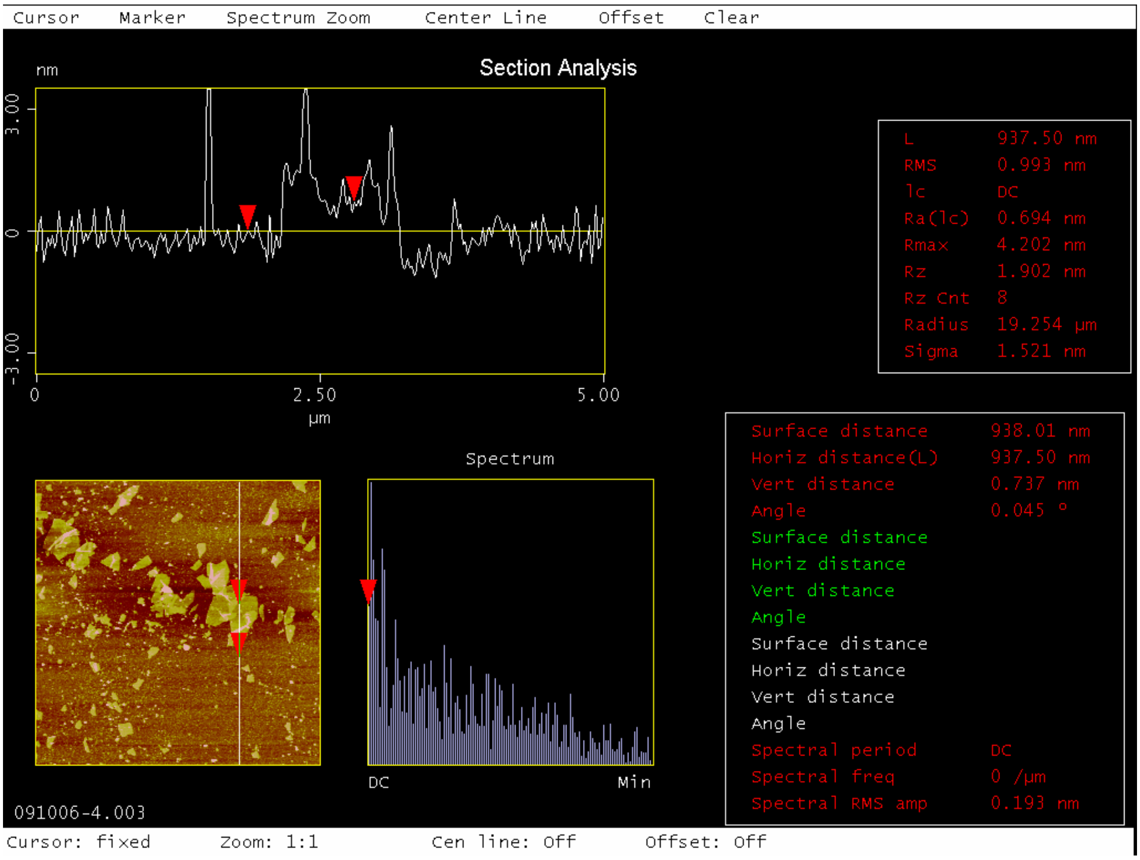

L	937.50 nm
RMS	0.993 nm
lc	DC
Ra(lc)	0.694 nm
Rmax	4.202 nm
Rz	1.902 nm
Rz Cnt	8
Radius	19.254 µm
Sigma	1.521 nm

Surface distance	938.01 nm
Horiz distance(L)	937.50 nm
Vert distance	0.737 nm
Angle	0.045 °
Surface distance	
Horiz distance	
Vert distance	
Angle	
Surface distance	
Horiz distance	
Vert distance	
Angle	
Spectral period	DC
Spectral freq	0 /µm
Spectral RMS amp	0.193 nm

Cursor: fixed Zoom: 1:1 Cen line: Off Offset: Off

Fig. S10 The AFM analysis of GO prepared by modified Hummers' method. The substrate is Si wafer. From this figure, the thickness of GO nanosheet equal to ca. 0.74 nm reveals the successful preparation of an isolated single-layer GO.

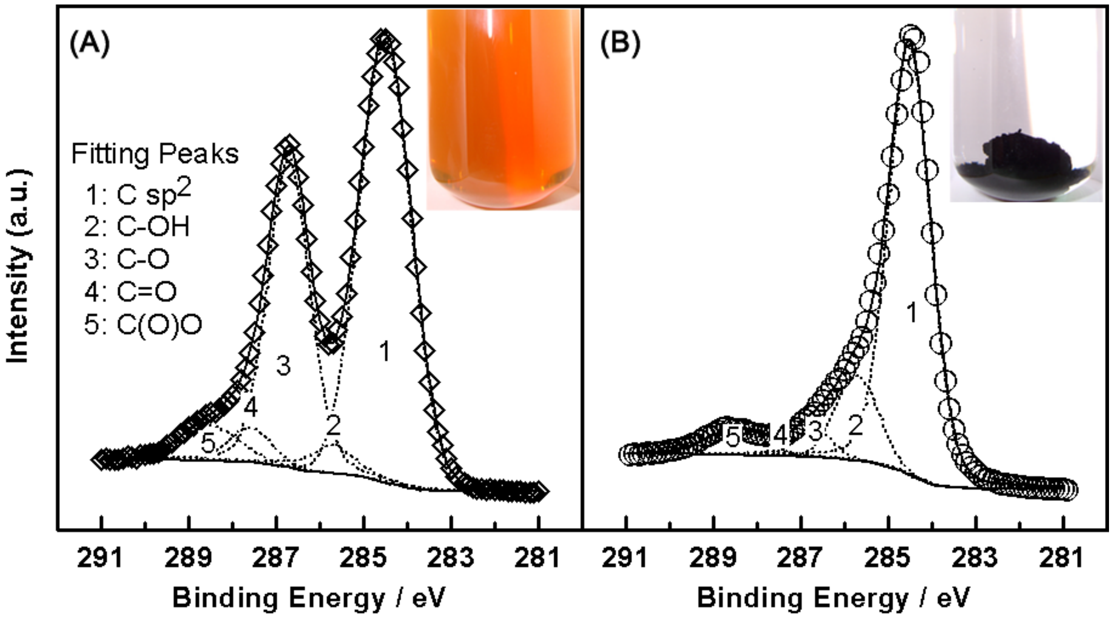

Fig. S11 The XPS C1 spectra of (A) GO and (B) reduced GO by microwave-assisted hydrothermal treatment at 200°C for 5 min. Insets are the corresponding photos of products. The XPS results and photos clearly prove the rapid removal of oxygen-containing functional groups from GO to form GS by microwave-assisted hydrothermal treatment at 200 °C for 5 min.